



OPEN

SUBJECT AREAS:
MINERALOGY
PALAEOCLIMATEReceived
5 February 2014Accepted
27 June 2014Published
22 July 2014Correspondence and
requests for materials
should be addressed to
H.Z. (zhhdut@163.
com)

Late Eocene to early Oligocene quantitative paleotemperature record: Evidence from continental halite fluid inclusions

Yan-jun Zhao¹, Hua Zhang¹, Cheng-lin Liu¹, Bao-kun Liu², Li-chun Ma¹ & Li-cheng Wang¹¹Ministry of Land and Resource (MLR) Key Laboratory of Metallogeny and Mineral Assessment, Institute of Mineral Resources, Chinese Academy Of Geological Sciences (CAGS), Beijing, 100037, China, ²China University of Geosciences, Beijing, 100083, China.

Climate changes within Cenozoic extreme climate events such as the Paleocene–Eocene Thermal Maximum and the First Oligocene Glacial provide good opportunities to estimate the global climate trends in our present and future life. However, quantitative paleotemperatures data for Cenozoic climatic reconstruction are still lacking, hindering a better understanding of the past and future climate conditions. In this contribution, quantitative paleotemperatures were determined by fluid inclusion homogenization temperature (T_h) data from continental halite of the first member of the Shahejie Formation (SF1; probably late Eocene to early Oligocene) in Bohai Bay Basin, North China. The primary textures of the SF1 halite typified by cumulate and chevron halite suggest halite deposited in a shallow saline water and halite T_h can serve as an temperature proxy. In total, one-hundred-twenty-one T_h data from primary and single-phase aqueous fluid inclusions with different depths were acquired by the cooling nucleation method. The results show that all T_h range from 17.7°C to 50.7°C, with the maximum homogenization temperatures (T_{hMAX}) of 50.5°C at the depth of 3028.04 m and 50.7°C at 3188.61 m, respectively. Both the T_{hMAX} presented here are significantly higher than the highest temperature recorded in this region since 1954 and agree with global temperature models for the year 2100 predicted by the Intergovernmental Panel on Climate Change.

Global warming and cooling is the most important environmental problem currently faced by humans. The trigger mechanisms and evolutionary processes of climate change always have been a focus for geoscientists. The Mesozoic and Cenozoic eras are considered to be one of the most important turning points of climate change when Earth's systems transitioned from the middle Cretaceous–early Paleogene typical “green house” conditions to “ice house” conditions after the middle–late Paleogene¹. Several extreme climate events, such as the Paleocene–Eocene Thermal Maximum (PETM, 55 Ma)², the First Oligocene Glacial (Oi-1; the Eocene–Oligocene, 33.5 Ma)³ and the First Miocene Glacial (Mi-1; Oligocene–Miocene, about 23 Ma), have been discovered during this interval. The proposed causes of those events include CH₄ gas eruption^{4,5}, volcanic activities⁶, changes in ocean current patterns⁷, and astronomical factors⁸. The drastic climate changes during this interval may be the best analogs for predicting future climate change on Earth^{9–11}, however, quantitative paleotemperature data are still lacking, posing an obstacle to further understanding of those events.

The continental and oceanic configuration during the middle–late Eocene was very similar to modern conditions¹², therefore climatic changes during this interval can provide an analogue for predicting the evolution of future climate. Fortunately, the Bohai Bay Basin, North China has not experienced significant change in latitude for the past 65 Ma^{13,14}, which offers us an good opportunity to peer into past and future climate conditions.

The Bohai Bay Basin is one of the most important oil and gas basins in China and hosted thick evaporite depositions during the Paleogene. Previous paleotemperature studies in this region mainly focused on palynology and indicated climate conditions changed from dry-hot to warm-humid from the fourth to first members of the Shahejie Formation (Eocene to Oligocene) as suggested by Li et al.¹⁵ and Xi et al.¹⁶. Detailed research on the first member of the Shahejie Formation (SF1) indicated a climate shift from cool to warm to cool again¹⁷, and this change of climate is closely related to the formation of oil and gas source rock in the Bohai Bay Basin^{17,18}.

The T_h of fluid inclusions in halite is closely related to the water or air temperature during deposition. This paper quantitatively determines paleoclimate characteristics by analyzing the T_h of primary, single-phase

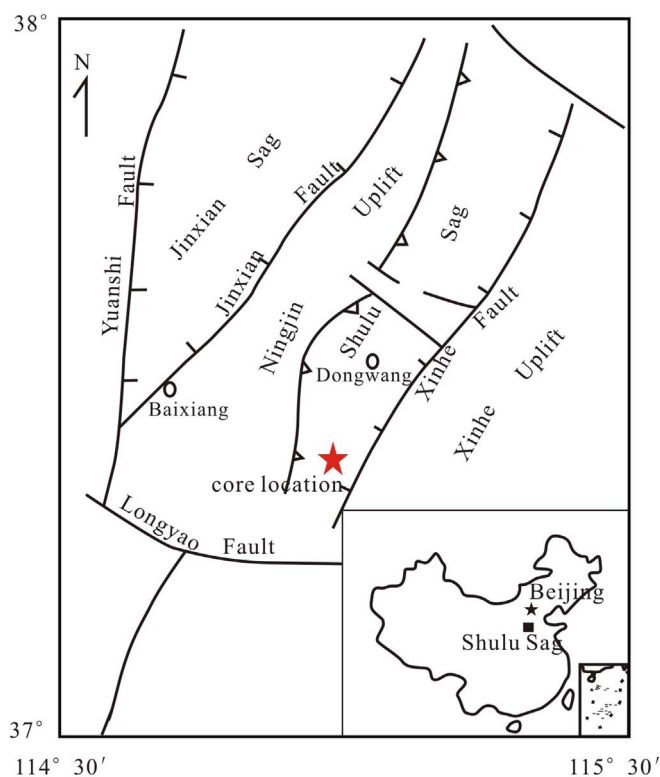


Figure 1 | Simplified structural map and location of the study area, the figure was produced using a base map of ref. 26 and 27.

aqueous fluid inclusions from halite in SF1 (probably late Eocene to early Oligocene). We used the cooling nucleation method to directly measure deposition temperatures of halite. This method has been proven to be very effective and has been widely used in reconstructing ancient climate from different geologic time periods, including Precambrian¹⁹, Permian^{20,21}, Eocene¹¹, Quaternary²², and modern²³. In addition, a series of experiments^{21,22,24,25} has demonstrated that the maximum homogenization temperature (Th_{MAX}) of halite fluid inclusions can represent the highest temperature of the water body in which the halite deposited and faithfully reflect the ancient climate. Thus, we chose Th_{MAX} from all samples in SF1 as a record of paleotemperatures in the Shulu Sag during this time.

The Shulu Sag is located on the southern edge of the Jizhong Depression of the Bohai Bay Basin (North China), and surrounded by the Hengshui and Xinghe Faults on its northern and eastern margins, and the Ningjin and Xiaoniuchun uplifts along its western and southern margins (Fig. 1). It is a typical half graben-like fault basin^{26,27} formed during the Eocene. Halite samples were collected from drill core in the southern Shulu Sag (Fig. 1) and preserved well since there were few volcanic thermal fluid events during the Paleogene to Neogene²⁸.

The Shahejie Formation can be divided into four members (SF1, SF2, SF3, SF4) from bottom to top, based on petrologic characteristics (Table 1). The SF1 is late Eocene to early Oligocene in age and consistent with the First Oligocene Glacial (Oi-1) in time. During the deposition of SF1, the Shulu Sag was separated by two uplifts into three sub-sags from north to south. The sub-sag where the study borehole located was a typical continental saline lake with high salinity²⁹.

The SF1 discussed in this study is characterized by evaporite sequences consisting of thin clastic layers shaped like bamboo kont (dark-gray mudstone or shale) and argillaceous limestone (Fig. 2). Halite in SF1 occurs in beds within which primary sedimentary structures or textures are well preserved (Figs. 3A and 3B). Chevron or cumulate crystals are widespread (Figs. 3C and 3D) and of which no deformation has been observation. All the evidences suggest that halite samples used in this paper are not altered and their Th values can be good climate proxies.

Results

Primary fluid inclusions in SF1 halite occur in chevron- or cumulate-type crystals (Fig. 4). Chevron crystals typically form at the bottom of saline lakes with depths less than 60 cm³⁰, so the Th of fluid inclusions in these crystals is analogous to ancient air temperatures^{11,21–23,25,31}. Cumulate crystals usually form at the air–water interface^{20,21,23} and sink to the bottom under gravity. If cumulate crystals occur in the same beds with chevron crystals, the Th of the two types of fluid inclusions can be used to study ancient air temperatures^{11,19–22,31}. Chevron and cumulate crystals were found in both samples B493 and B1003, which indicates that the halite studied here was deposited in shallow water and the Th of fluid inclusions can be used to interpret paleoenvironmental conditions.

In total, about 360 pieces of halite from samples B493 and B1003 have been observed in detail and only 38 pieces of halite are available to Th analysis due to primary fluid inclusion in most of the halite pieces are few or absent. The Size of primary fluid inclusions (both of cumulate and chevron crystals) range from 2 to 20 μ m and up to 40 to 50 μ m. Primary fluid inclusions coexist in both single liquid and gas-liquid phases, and only the single-phase liquid fluid inclusions are chose for Th analysis. The Th of halite fluid inclusion was tested with the cooling nucleation method, and the results are shown in Table 2.

Sample B493: Sixty-one Th data of primary and single-phase aqueous fluid inclusions were obtained (Fig. 5A). Th values of sample B493 range from 24.4°C to 50.5°C and with the average homogenization temperature (Th_{AVG}) of 39.8°C. Thirteen Th values were obtained from fluid inclusions in chevron crystals with Th_{AVG} of 39.9°C, Th_{MIN} of 24.4°C, and Th_{MAX} of 50.5°C. Forty-eight Th values were obtained from fluid inclusions in cumulate crystals, with Th_{AVG} of 39.7°C, Th_{MIN} of 29.5°C, and Th_{MAX} of 49.6°C. Sample B1003: Sixty-one Th values were obtained (Fig. 5B). Th values of this sample range from 17.7°C to 50.7°C, with the Th_{AVG} of 37.3°C Seven Th values were obtained from fluid inclusions in chevron crystals,

Table 1 | stratigraphic characteristics of the Shahejie Formation in Shulu Sag, Bohai Bay Basin, North China

Geological time	Formation	Thickness (m)	Lithology
Oligocene	SF 1	0 ~ 800	The lower part: red and black mudstone, carbonate, gypsum, argillaceous gypsum and salt rock, From north to south in the southern part of the depression, the lithology was marked by limestone - dolomite - gypsum – halite
Eocene	SF 2	0 ~ 400	The upper part: light grey fine sandstone, siltstone and amaranth mudstone interbedded brown, purple mudstone and light grey fine sandstone brown and grey breccia, breccia composed mainly of limestone or dolomite, brownish gray, grey mudstone, local shale and grayish fine sandstone in the upper
	SF 3	0 ~ 2200	
	SF 4	500 ~ 1000	
			Clastic sediments mainly developed around the periphery of the basin, and mudstone sedimentary rocks and mud paste emerged in the center of the depression

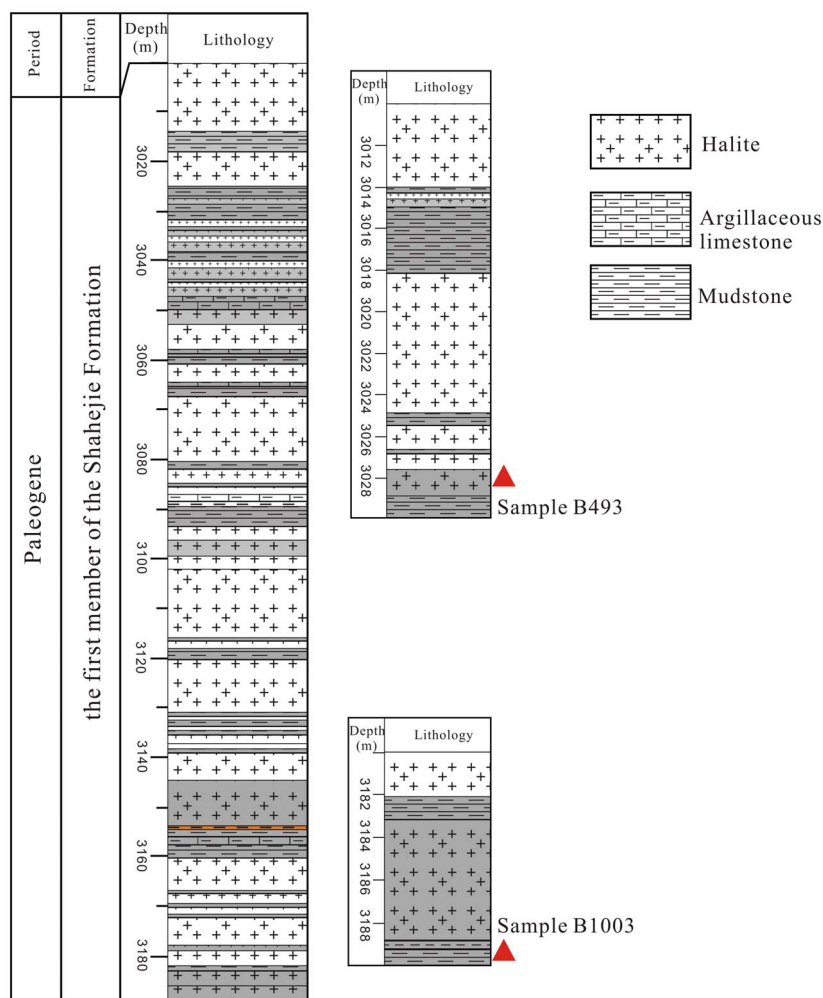


Figure 2 | Lithology of the first member of Shahejie Formation (SF1), Shulu Sag, Bohai Bay Basin.



Figure 3 | Macrofeature of SF 1 in Shulu Sag, Bohai Bay Basin. (A) and (B), The primary rhythmical textures in evaporite sequence are characterized by the alternating thin clastic beds shaped like 'bamboo knot' and thick halite bed. (C) (sample B493, 3028.04 m) and (D) (B1003, 3188.61 m), Halite occur in particles and are often overgrown by halite cements.

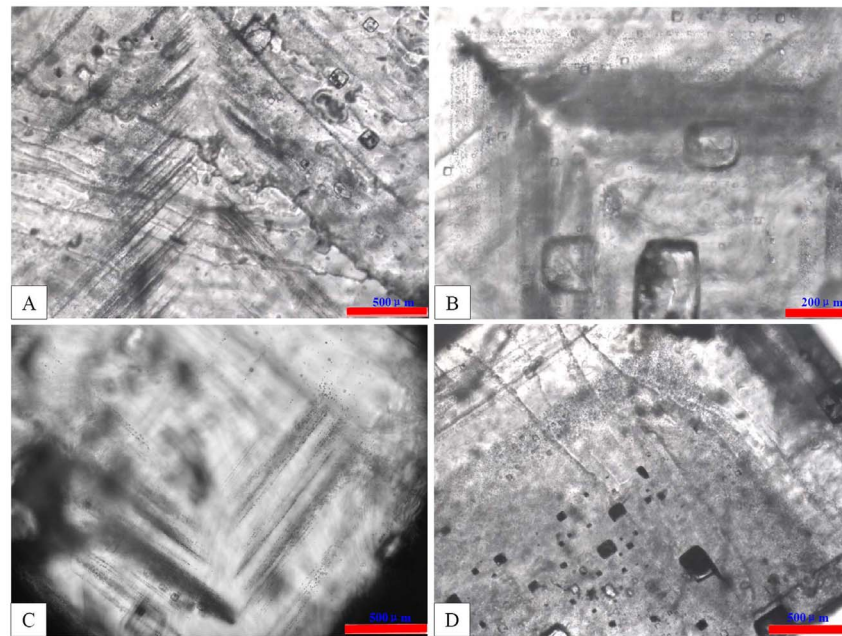


Figure 4 | Primary fluid inclusions in SF 1 halite in the Shulu Sag. (A)-photomicrograph of primary fluid inclusions in chevron halite of sample B493; (B)-Photomicrograph of primary fluid inclusions in cumulate halite of sample B493; (C)-photomicrograph of primary fluid inclusions in chevron halite of sample B1003; (D)-Photomicrograph of primary fluid inclusions in cumulate halite of sample B1003.

with Th_{AVG} of 41.7°C, Th_{MIN} of 38.8°C and Th_{MAX} of 42.8°C. Fifty-four Th values were obtained from fluid inclusions of cumulate crystals, with Th_{AVG} of 37.0°C, Th_{MIN} of 17.7°C and Th_{MAX} of 50.7°C.

Discussion

Changes of Th values from the same sample or even the same inclusion band may be caused by seasonal or diurnal temperature fluctuations^{20,23}. Consensus is that the Th_{MAX} of single liquid phase

Table 2 | Th statistics of fluid inclusions in SF 1 halite

Sample number	Types of crystals	Data of Th (°C)	Th_{MAX} (°C)	Th_{MIN} (°C)	Th_{AVG} (°C)	Th_{MEDIAN} (°C)
B493	chevron	24.4;35.2;35.4;35.6;36.3; 37.3;38.3;41.5;43.7; 44.5; 47.9;48.0;50.5	50.5	24.4	39.9	38.3
	cumulate	29.5;31.7;33.3;33.4;33.5; 33.7;33.8;34.5;34.7; 34.9; 36.5;36.7;36.8; 36.9;37.2; 37.2;37.2; 37.8;38.2;38.3; 38.5; 38.5;38.8;38.9;39.7; 39.7;40.5;40.6;40.6; 40.9; 41.0;41.1;41.6; 41.7;41.8; 42.0;42.4; 43.5;43.9;44.9; 45.7; 46.2;47.6;47.6;47.7; 47.8;48.0;49.6	49.6	29.5	39.7	39.3
B1003	chevron	38.8;8.9;49.1;48.1;46.3; 37.6;42.8	42.8	38.8	41.7	48.1
	cumulate	17.7;28.7;29.1;30.0;30.1; 30.2;30.2;32.5;33.0; 33.3; 33.5;34.3;34.5; 34.6;34.6; 34.8;34.9; 35.2;35.2;35.2; 35.6; 36.0;36.0;36.2;36.6; 36.8;37.2;37.2;37.2; 37.3; 37.5;37.5;37.5; 37.7;38.3; 38.5;38.5; 38.6;38.8;39.0; 39.3; 39.8;40.6;40.6;41.2; 41.3;41.9;43.6;43.7; 44.5; 44.6;46.3;48.3;50.7	50.7	17.7	37.0	37.2

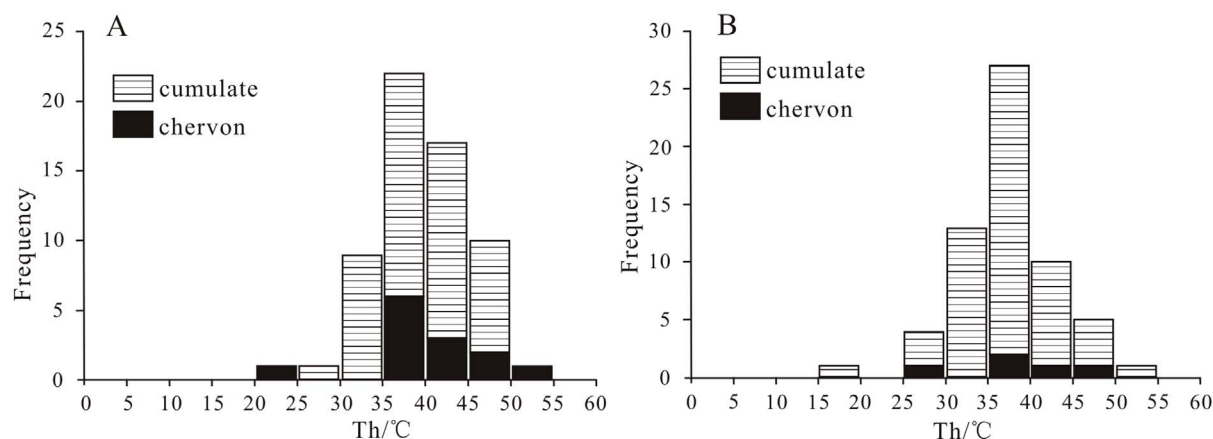


Figure 5 | Histogram of homogenization temperature plotted against number of fluid inclusions. (A) -sample B493, 61 Th data of primary fluid inclusions; (B)-sample B1003, 61 Th data of primary fluid inclusions.

inclusions can represent the highest brine temperature both at the bottom and at the air–water interface^{11,22,25}.

The ranges of Th are different from chevron and cumulate crystals from sample B1003 because the number of fluid inclusions in chevron crystals is smaller than that in cumulate crystals. However, the range and average values of Th from these two types of halite crystals in sample B493 are very similar. The Th from both samples characterized by normal distribution, and co-occurrence of chevrons and cumulates in the same beds suggests the Th is valid and representative. The Th values indicate that the water temperature of ancient salt lakes ranged from 17.7 to 50.7°C, and ancient air temperatures had corresponding changes in this region.

As mentioned earlier, the Th_{MAX} of single-phase, aqueous fluid inclusions represents the highest air temperature during halite deposition. The Th_{MAX} in Shulu Sag during formation of SF1 is 50.7°C, which is 9.2°C higher than the highest temperature recorded since 1954 in this region (local temperature data, and Wu et al.³²). Given that the Th_{MAX} of single-phase aqueous fluid inclusions in halite from modern salt lakes is slightly (less than 5°C) higher than the air temperature^{33,34}, we infer that paleotemperatures during deposition of the SF1 were at least 4.2°C higher than the temperatures of the past 60 years. Because the study area has not significantly displaced over the last 65 Ma^{13,14} and the Th_{MAX} values of these two samples (sampling interval is about 160 m) are very similar, we speculate that the higher temperatures state evidenced by Th of halite fluid inclusion in the Shulu Sag may last a considerable time. Combining with the Eocene paleotemperature data from other places in China¹¹, it implies that higher temperatures were widespread in

eastern China during this interval. This phenomenon of higher temperature is well correlated with the occurrence of large-scale evaporite deposits in the same area during that time. In addition, the average temperature in China has risen by 0.5–0.8°C over the past 100 years³⁵, while global temperatures are predicted to rise 1.4–5.8°C by 2100^{11,36}. This study of homogenization temperatures of fluid inclusions from mid and late Eocene halite in Hubei, China, also indicates that paleotemperatures at the time were 4.6°C higher than today's temperatures¹¹. Therefore, it can be predicted that climate warming will continue and not be reversed in the short term.

Methods

Halite samples were collected from two depths (Fig. 2; 3028.04 m, sample number B493 and 3188.61 m, sample number B1003). Before determining the Th of fluid inclusions, halite samples were chosen by XRD (D/max-rA12kw, Rigaku Corporation, Japan). Temperature information is susceptible to distortion due to alteration of halite fluid inclusions by dissolution or heating during sawing. We referred to the methods outlined in Roberts and Spencer²³, Lowenstein et al.²², Benison and Goldstein²⁰ and split the halite samples with a hammer and chisel along cleavage planes, into fragments with thicknesses of 0.5 to 1 mm. All the halite fragments were so smooth that changes to the fluid inclusions could be monitored under a microscope during heating and cooling. We observed and photographed these cleavage flakes under the microscope, and documented the occurrence and morphology of primary fluid inclusions. Halite samples were then sealed in self-sealing plastic bags and put into an airtight plastic box. Desiccant was added to the box for moisture protection, and the box was then transferred into a Haier freezer for about 1 week (multiple measurements showed that the temperature was stable at −18°C). After the single-phase fluid inclusions were frozen to nucleate bubbles (Fig. 6), we measured Th using a Linkam THMSG600 heating and cooling stage. The heating rate of the stage was first set at 0.5°C/min, but was lowered to 0.1–0.2°C/min when approaching 20°C.

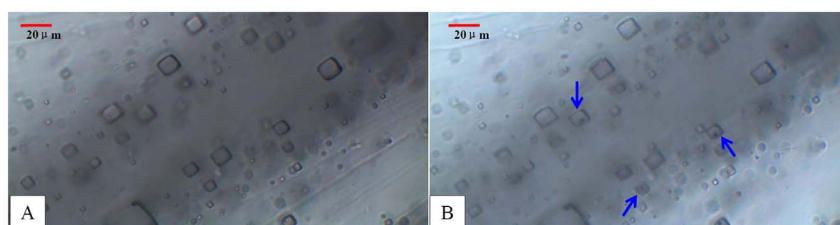


Figure 6 | Change of fluid inclusions during the ‘cooling nucleation’ process. (A)-primary fluid inclusion without vapor bubble at room temperature; (B)-Vapor bubble formed within primary fluid inclusions after cooling.



1. Jiang, T., Jia, J. Z., Deng, L. J. & Wan, X. Q. Significant climate events in Paleogene and their biotic response. *Geol. Sci. Tech. Inf.* **31**, 31–38 (2012).
2. Wing, S. L. & Greenwood, D. R. Fossils and fossil climate: the case for equable continental interiors in the Eocene. *Philos. T. Roy. Soc. B.* **341**, 243–252 (1993).
3. Bralower, T. J., Silva, I. P. & Malone, M. J. New evidence for abrupt climate change in the Cretaceous and Paleogene: An ocean drilling program expedition to Shatsky Rise, northwest Pacific. *GSA Today* **11**, 4–10 (2002).
4. Zachos, J. C., Rohl, U. & Schellenberg, S. A. Rapid acidification of the ocean during the Paleocene-Eocene thermal maximum. *Science* **308**, 1611–1615 (2005).
5. Bowen, G. J. & Zachos, J. C. Rapid carbon sequestration at the termination of the Palaeocene-Eocene thermal maximum. *Nat. Geosci.* **3**, 866–869 (2010).
6. Kent, D. V. *et al.* Reply to a comment on “A case for a comet impact trigger for the Paleocene/Eocene thermal maximum and carbon isotope excursion” by Dickens, G.R. and Francis, J.M. *EPSL* **211**, 13–26 (2003).
7. Ge, X. H. *et al.* Multi-stage uplifts of the Qinghai-Tibet plateau and their environmental effects. *Earth Sci. Front.* **13**, 118–130 (2006).
8. Zachos, J. C., Shackleton, N. J., Revenaugh, J. S., Palike, H. & Flower, B. P. Climate response to orbital forcing across the Oligocene-Miocene boundary. *Science* **292**, 274–278 (2001).
9. Bowen, G. J. *et al.* Eocene hyperthermal event offers insight into greenhouse warming. *EOS, Trans. AGU* **87**, 165–169 (2006).
10. Pagani, M., Caldeira, K., Archer, D. & Zachos, J. C. An ancient carbon mystery. *Science* **314**, 1556–1557 (2006).
11. Meng, F. W. *et al.* Choosing the best ancient analogue for projected future temperatures: A case using data from fluid inclusions of middle-late Eocene halites. *J. Asian Earth Sci.* **67–68**, 46–50 (2013).
12. Boucot, A. J., Chen, X., Scotese, C. R. & Fan, J. X. *Phanerozoic Global Paleoclimatic Reconstructions*. [136–148] (Science Press 2009).
13. Cheng, G. L., Sun, Y. H. & Li, S. L. China paleomagnetic data list for Cenozoic. *Seismol. Geol.* **13**, 184–186 (1991).
14. Wan, T. F. & Zhu, H. Tectonics and environment change of Meso-Cenozoic in China continent and its adjacent areas. *Geoscience* **16**, 107–120 (2002).
15. Li, S. J., Wang, M. Z., Zheng, D. S. & Zhao, X. L. Recovery of climate of Palaeogene in Jiyang Depression of Shandong. *J. Shandong Univ. Sci. Technol. (Nat. Sci.)* **22**, 6–9 (2003).
16. Xi, Z. G., Guo, J. X. & Zhao, X. Y. Palaeoecological analysis of Paleogene Shahejie Formation in north central Raoyang Sag of central Hebei Depression. *J. Earth Sci. Environ.* **33**, 358–363 (2011).
17. Wang, G. M. & Lin, G. S. Eocene paleoclimate zone study in the Jiyang Depression. *Bull. China Soc. Mineral. Petrol. Geochem.* **31**, 505–509 (2012).
18. Liu, Z. H., Li, S. T., Xin, R. C., Xu, C. G. & Cheng, J. C. Paleoclimatic information in stratigraphic records and its relation to the formation of hydrocarbon source rocks—A case study of the Paleogene strata in the Huanghekou subbasin of the Bohai Bay basin, China. *Geol. Bull. China* **26**, 830–840 (2007).
19. Meng, F. W. *et al.* Ediacaran seawater temperature: evidence from inclusions of Sinianhalite. *Precambrian Res.* **184**, 63–69 (2011).
20. Benison, K. C. & Goldstein, R. H. Permian paleoclimate data from fluid inclusions in halite. *Chem. Geol.* **154**, 113–132 (1999).
21. Zambito IV, J. J. & Benison, K. C. Extremely high temperatures and paleoclimate trends recorded in Permian ephemeral lake halite. *Geology* **41**, 587–590 (2013).
22. Lowenstein, T. K., Li, J. R. & Brown, C. B. Paleotemperatures from fluid inclusions in halite: Method verification and a 100000 year paleotemperature record, Death Valley, CA. *Chem. Geol.* **150**, 223–245 (1998).
23. Roberts, S. M. & Spencer, R. J. Paleotemperatures preserved in fluid inclusions in halite. *Geochim. Cosmochim. Acta* **59**, 3929–3942 (1995).
24. Liu, X. Q. & Ni, P. Advances in studies of fluid inclusions in halite formed in earth's surface environments. *Adv. Earth Sci.* **20**, 856–862 (2005).
25. Meng, F. W. *et al.* Homogenization temperature of fluid inclusions in laboratory grown halite and its implication for paleotemperature reconstruction. *Acta Petrol. Sin.* **27**, 1543–1547 (2011).
26. Kong, D. Y., Shen, H., Liu, J. Y. & Yin, W. Origin of transverse accommodation zone of the Shulu subbasin in the Jizhong Depression. *Chin. Geol.* **32**, 690–695 (2005).
27. Wang, C. Y., Zhang, X. K., Lin, Z. Y. & Li, X. Q. Crustal structure in Shulu fault basin and its adjacent areas. *Acta Seism. Sin.* **16**, 472–479 (1994).
28. Peng, N. *et al.* Tertiary volcanic lithofacies characteristics and oil-gas reservoir accumulation model, Jizhong depression. *Pet. Geol. Recov. Effic.* **17**, 17–20 (2010).
29. Chen, D. Q. Seismic facies, sedimentary facies and hydrocarbon accumulation conditions of Shulu Sag. *Master's thesis of Univ. Pet. China* [1–33] (Univ. Pet. China 1985).
30. Handford, C. R. Halite depositional facies in a solar salt pond: A key to interpreting physical energy and water depth in ancient deposits? *Geology*, **18**, 691–694 (1990).
31. Roedder, E. The fluids in salt. *Am. Mineral.* **69**, 413–439 (1984).
32. Wu, Z. J., Xu, X. L. & Wang, C. M. Change characteristics of season length and extreme temperature of Xintai City in recent 57 years. *J. Anhui Agri. Sci.* **39**, 18180–18184 (2011).
33. Lowenstein, T. K. & Brennan, S. T. [Fluid inclusions in paleolimnological studies of chemical sediments tracking environmental change using lake sediments] *Developments in Paleoenvironmental Research*, [Last, W. M., Smol, J. P. & Birks, H. J. B. (eds.)] [189–216] (Springer Netherlands 2002).
34. Liu, X. Q., Ni, P., Dong, H. L. & Wang, T. G. Homogenization temperature and its significance for primary fluid inclusion in halite formed in Chaka salt lake, Qardam basin. *Acta Petrol. Sin.* **23**, 113–116 (2007).
35. Qin, D. H. *et al.* Updated understanding of climate change sciences. *Adv. clim. change res.* **3**, 63–73 (2007).
36. IPCC (Intergovernmental Panel on Climate Change) [Climate Change 2001] *The Science of Climate Change* [Cambridge University Press 2001].

Acknowledgments

This study was supported by National Natural Science Foundation of China (No. 41302059) and Major State Basic Research Development Program (No.2011CB403007).

Author contributions

Y.J.Z., H.Z., C.L.L. and L.C.M. designed the research in the manuscript. B.K.L. and L.C.W. have been an active participant in the sample collection and processing. Y.J.Z. and H.Z. wrote the manuscript and prepared all figures. All authors reviewed the manuscript.

Additional information

Competing financial interests: The authors declare no competing financial interests.

How to cite this article: Zhao, Y.-J. *et al.* Late Eocene to early Oligocene quantitative paleotemperature record: Evidence from continental halite fluid inclusions. *Sci. Rep.* **4**, 5776; DOI:10.1038/srep05776 (2014).



This work is licensed under a Creative Commons Attribution 4.0 International License. The images or other third party material in this article are included in the article's Creative Commons license, unless indicated otherwise in the credit line; if the material is not included under the Creative Commons license, users will need to obtain permission from the license holder in order to reproduce the material. To view a copy of this license, visit <http://creativecommons.org/licenses/by/4.0/>